Journal of Alloys and Compounds 924 (2022) 166531

Contents lists available at ScienceDirect

Journal of Alloys and Compounds

journal homepage: www.elsevier.com/locate/jalcom

Optimization of active antireflection ZnO films for p-GaAs-based heterojunction solar cells

Thi Kim Oanh Vu[a,*], Minh Tien Tran[a], Eun Kyu Kim[b,*]

[a] Institute of Physics, Vietnam Academy of Science and Technology, No. 10 Dao Tan, Viet Nam
[b] Department of Physics and Research Institute for Natural Sciences, Hanyang University, Seoul 04763, the Republic of Korea

ARTICLE INFO

Article history:
Received 27 January 2022
Received in revised form 22 July 2022
Accepted 26 July 2022
Available online 27 July 2022

Keywords:
ZnO films
P-GaAs
Heterojunction solar cells
Oxygen pressure

ABSTRACT

We have optimized the photovoltaic properties of active ZnO/p-GaAs heterojunction solar cells by pulsed laser deposition method by varying the oxygen pressure from 0 to 50 mTorr during the fabrication process. We observed the crystallinity and grain size of ZnO enhanced with increasing oxygen pressure from 0 to 30 mTorr. In addition, with this increase of oxygen flux, the intensity of $E_1(LO)$ modes obtained by Raman measurements declines significantly and almost disappears under an oxygen pressure of 50 mTorr. The change of intensity is assumed to be the change of oxygen vacancy and zinc interstitial concentrations in ZnO films with oxygen pressures. Current-voltage measurements and extractions show that ZnO grown at 30 mTorr displays the best performance with the I_{SC} of 24.3 mA/cm^2, the efficiency of 8.746 %, and FF_0 of 68.73 %. The high performance of the heterojunction solar cell grown at the oxygen partial pressure of 30 mTorr might be due to the reduction of oxygen vacancies by increasing oxygen during the deposition. The results reveal the importance of the oxygen processing gas in promoting devices performance.

1. Introduction

Interest in the renewable sector has grown enormously in the last few years due to emphasis on environmental and climate change issues. The global eventually is going to run out of coal and gas, most governments are focusing on the growth of alternative sources of energy. Therefore the manufacturing of photovoltaic (PV) devices has developed considerably in recent decades, spurred by continuous growth in the demand for the renewable energy sources. Photovoltaic power generation employs solar panels composed of several solar cells containing photovoltaics materials. At present, silicon solar cells dominate 95 % in the photovoltaic market [1], and crystalline silicon solar cells approach an efficiency of 29.43 % theoretically [2]. However, the spectra response of the Si PV device does not match the solar emission spectrum owing to the limited absorption of Si constituting the PV solar cell active layer. A single-junction Si solar cell is transparent to photons with energies below band gap energy, and additional sunlight is lost because of thermal induce. To overcome this problem and reduce the production cost, currently, lead halide perovskite solar cells have become a star in photovoltaic research [3–5] and achieved a high efficiency surpassing the 25 % mark in 2020 [6]. Despite of impressive high performance, perovskite solar cells have faced challenges of long-term durability that inhibit their practical uses. Therefore, optimizing well-known GaAs-based solar cells is still a long-term strategy. GaAs possesses more outstanding characteristic than Si including light absorption coefficient is about 10^4 times lower than Si that 10–100x thinner GaAs layer is required to absorb the same amount of light in comparison with Si [7,8].

For achieving friendly environmental and high-efficiency GaAs-based solar cells, a new approach by depositing ZnO thin films on the surface of solar cells has recently been proposed [9,10]. ZnO has a direct wide band gap of 3.3 eV [11] at room temperature that is associated with higher breakdown voltage, ability to sustain large electric field, lower electric noise, and high-temperature and high-power operation. ZnO owns unique characteristics compared to other II-VI wide bandgap materials such as low cost, low toxicity, and larger exciton binding energy of 60 meV [12] which guarantees efficient photovoltaic properties. In addition, ZnO is transparent in the visible and infrared regions, which is one of the most important properties of its antireflection coating application on solar cells. Due to these characteristics, fabricating high-quality ZnO thin films are emerged solutions to improve the efficiency of GaAs-based solar cells.

* Corresponding authors.
E-mail addresses: oanhvtk@iop.vast.vn (T.K. Oanh Vu), ek-kim@hanyang.ac.kr (E.K. Kim).

https://doi.org/10.1016/j.jallcom.2022.166531
0925-8388/

In this study, we optimized the quality of ZnO thin films and the performance of n-ZnO/p-GaAs heterojunction solar cells. ZnO thin films were deposited on the p-GaAs substrate by pulsed laser deposition (PLD) methods to well-control oxygen working pressure from 0 to 50 mTorr and substrate temperature. The merits of using PLD were reported in our previous works of literature [13,14]. The structural characteristics and optical properties of n-ZnO/p-GaAs heterojunctions were evaluated using X-ray diffraction (XRD), atomic force microscopy (AFM), and Raman spectrum. Current-voltage measurements were carried out for the evaluation of photovoltaic properties. The ZnO layers were found to be an excellent antireflection coating and to exhibit exceptional light-trapping at wavelengths ranging from 365 to 800 nm, which led to a high efficiency of p-GaAs solar cell of 8.746 % at 30 mTorr. Moreover, we demonstrated that the ZnO/p-GaAs solar cell's quality can be well-controlled by oxygen partial pressure during the deposition process.

2. Experimental method

2.1. Sample preparation

The p-GaAs substrates were cleaned in acetone and methanol followed by rinsing in deionized water. Each step was conducted for 15 min, and then GaAs wafers were dried under the flux of compressed nitrogen. ZnO thin films were grown on the GaAs substrates by using Pulsed Laser Deposition (PLD) method. High purity ZnO (99.99 % purity) target was used to deposit thin films. The experiments were performed in a vacuum chamber. After the GaAs substrate was loaded into the chamber, the vacuum chamber was evacuated by a turbo-molecule pump in eight hours until the vacuum pressure down to 10^{-7} Torr. An Nd-YAG laser was operated at a wavelength of 266 nm, energy density of 5 J/cm^2, and repetition rate of 10 Hz. The ZnO films were deposited under oxygen partial pressure varying from 0 to 50 mTorr. Depositing time and substrate temperature were 60 min and 300 °C, respectively. After deposition, the film was then allowed to cool to room temperature before carrying out the structural, morphology, and optical measurements. To fabricate n-ZnO/P-GaAs-based solar cells, two metal electrodes were deposited on ZnO and GaAs layer by thermal evaporation. The Ti/Au (20/50 nm) bilayers were grown on ZnO films and Au (70 nm) layers were deposited on GaAs wafers to form Ohmic contacts.

2.2. Characterizing methods

The structural properties of ZnO thin films grown on p-GaAs wafers were examined by a θ - 2θ rocking curve on a scanning XRD system using a Cu Kα wavelength of 0.15418 nm. The surface morphology and roughness of films were investigated using atomic force microscopy (AFM). Raman spectra were obtained by a Near-Field Scanning Optical Microscope imaging system integrated with a Raman spectrometer with continuous laser light of 532 nm. The I – V characteristic of n – ZnO/p – GaAs heterojunction solar cells were conducted under 1 sun illumination, whose intensity level was about 100 mW/cm^2 on the film surface. External Quantum Efficiency (EQE) was performed over UV to IR wavelengths (200–870 nm) using a Xe light source. The incident wavelength of the Xe light was resolved by a monochromator with a wavelength step of 1 nm.

3. Results and discussions

We have investigated the influence of the various oxygen pressure from 0 to 50 mTorr on the crystal structure of ZnO/p-GaAs. The

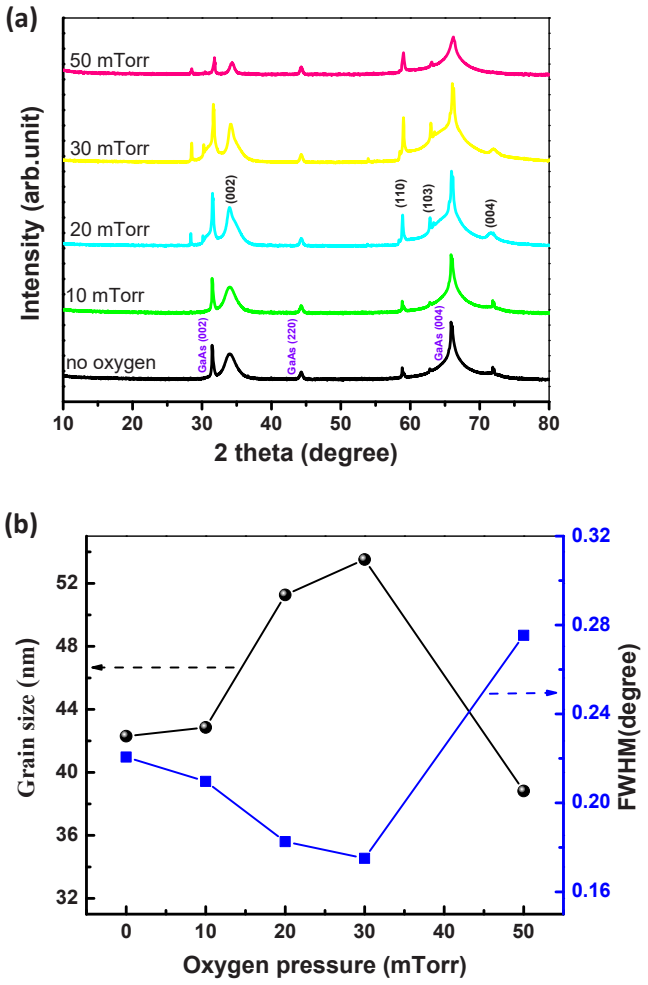

Fig. 1. (a) X-ray diffraction patterns of as-grown ZnO films grown on p-GaAs under various oxygen pressures. (b) FWHM and grain size of the (110) diffraction peak of ZnO films as a function of oxygen pressure.

XRD patterns of five samples under the different gas pressure are shown in Fig. 1(a). These data confirmed the polycrystalline nature of films grown at a temperature of 300 ℃ showing the main reflection characteristic of the ZnO wurtzite structure [15]. The XRD spectrum exhibited three noticeable peaks at 2θ values of 31.45°, 44.24°, and 66.01°, which correspond to the (002), (220), and (004) planes of p-GaAs, respectively. In addition, four significant peaks corresponding to ZnO films are observed at 34.01°, 58.68°, 62.93°, and 71.91°. According to the Joint Committee on Powder Diffraction Standards (JP 89-1397), these peaks are originated from the (002), (110), (103), and (004), respectively. It is shown clearly that the crystal orientation of the ZnO is dominantly by (002) and (110) planes. As the oxygen pressure increased, the (002) and (110) peaks intensity first increased and then decreased gradually. The intensity value reached a maximum at an oxygen pressure of 30 mTorr. The full width at half maximum (FWHM) of the (110) diffraction peak and the crystallite size extracted from the FWHM according to the Scherrer formula [16] for the ZnO films deposited at different oxygen pressures are given in Fig. 1(b). The value of FWHM decreased from 0.22° to 0.17° with increasing oxygen partial pressure up to 30 mTorr which indicated that the crystallinity of ZnO thin films improved up to oxygen partial pressure of 30 mTorr. This improvement of

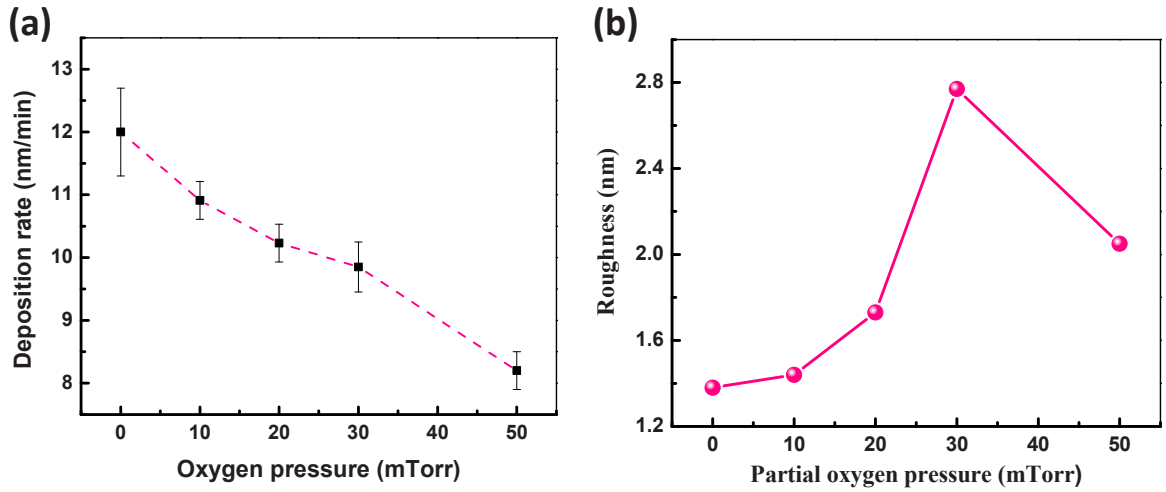

Fig. 2. (a) Evolution of the deposition rate and (b) (b) RMS roughness of ZnO thin films grown on p-GaAs substrates versus the oxygen pressure.

crystallinity with oxygen pressure could be attributed to the increase of a number of reactive oxygen ions and also the enhancement of interaction between zinc ions with oxygen ions in the chamber due to sufficient kinetic energy to the atoms on the substrate to move them to the suitable sites [17]. However, when increasing oxygen pressure from 30 to 50 mTorr, the XRD intensity reduced dramatically and FWHM grew sharply to 0.27° which indicated the degradation of crystallinity of thin films. It is assumed that the excess of oxygen might induce defects in the ZnO thin films, which influenced the nucleation and growth of the thin films, resulting in the degradation of the crystalline quality. Another possibility is the reduction of the mobility of ad-atoms to the energy favorable positions as increasing oxygen flux causes a decline of XRD intensity [18]. As the change of FWHM with oxygen flux, the crystallite size extracted from FWHM also changed. The calculated mean grain size enhanced from 42.3 nm at 0 mTorr to 53.5 nm at 30 mTorr and decreased down to 38.8 nm at 50 mTorr. The grain size of ZnO films was confirmed by AFM measurements. Therefore, the oxygen pressure is responsible for the change of the XRD diffraction, and both the mobility of the ablated species and the intrinsic defects concentration could be controlled by oxygen pressure during the deposition process.

The relation between the ZnO deposition rate and the oxygen working pressure during growth is presented in Fig. 2(a). The lowest rate is obtained (~ 8.2 nm/min) in the deposition process under an oxygen pressure of 50 mTorr. The growth rate of the films increases from 8.2 to 12 nm/min for reducing the oxygen pressure from 50 down to 0 mTorr, respectively. The different oxygen pressures can influence the growth rate due to their atom's energy. By using the pulse laser deposition method, at higher oxygen pressure, the ablated species could undergo more collision with the oxygen molecules leading to thermalizing the film-forming particles and decreasing the kinetic energy of these species, hence reduce the growth rate [19]. The different deposition rate as a function of oxygen pressure leads to the different thickness of ZnO films which directly affects the performance of n-ZnO/p-GaAs. Particularly, the thickness of ZnO films grown under an oxygen pressure of 0, 10, 20, 30, and 50 are about 720, 655, 613, and 492 nm, respectively. The root means square (RMS) roughness of ZnO films on GaAs substrates with various oxygen pressures is illustrated in Fig. 2(b). When we increase the oxygen flux from 0 to 30 mTorr, the surface roughness gradually increases from 1.36 to 2.77 nm and decreases to about 2 nm as oxygen pressure is raised to 50 mTorr. The increased grain size with the increase of oxygen pressure (from 0 to 30 mTorr) was the primary reason for the increase in the RMS roughness. However, the RMS roughness values for every sample are not too high, so the ZnO films grown by PLD are uniform naturally. The above XRD analysis and AFM images confirmed this result. Fig. 3(a–e) present the AFM images of ZnO thin films grown on GaAs substrate obtained at 300 ℃ under various oxygen pressures from 0 to 50 mTorr, respectively. As shown in the figures, the ZnO films are composed of a polycrystalline structure with random orientation grains. The particles size increase from 80 to 120 nm with increasing of partial oxygen pressure from 0 to 30 mTorr, and reduces down to about 90 nm at an oxygen pressure of 50 mTorr. The particle sizes observed in AFM images are higher than that estimated from XRD analysis could be ascribed to the formation of clusters from the deposited ad-atoms. The larger clusters lead to higher RMS roughness (Fig. 2(b)). The trend of changing the size of the cluster with the various oxygen pressures is similar to the calculated crystallite sizes extracted from XRD analysis. The XRD and AFM results suggest that the increase of oxygen flux resulted in changes in the crystal structure and morphology of ZnO thin films.

Moreover, oxygen pressure was discovered to influence the optical properties of ZnO films in this work. In the case of wurtzite ZnO, there are 12 phonon modes including 3 modes for acoustic phonon and 9 modes for optical phonon. Among 12 phonon modes, there are one longitudinal-acoustic (LO), 2 transverse-acoustic (TA), 3 longitudinal-optical (LO), and 6 transverse-optical (TO) branches. The zone-center optical phonons can be classified according the following relation: $\Gamma_{opt} = A_1 + E_1 + 2E_2 + 2B_1$, with B_1 are silent modes, A_1 and E_1 are polar modes, and E_2 are nonpolar and Raman active only [20]. Fig. 4(a) shows the Raman spectra of ZnO thin films deposited on a p-GaAs substrate with different oxygen pressure from 0 to 50 mTorr. As clearly presented in the figure, there are two intensive peaks located at about 299 cm^{-1} and 580 cm^{-1} which corresponds to the GaAs (LO) and ZnO E_1(LO) mode, respectively. Although all of the modes in ZnO films are influenced by impurities or defects, the E_1(LO) mode is more strongly affected by these effects, and this mode is directly related to oxygen vacancies [20]. As

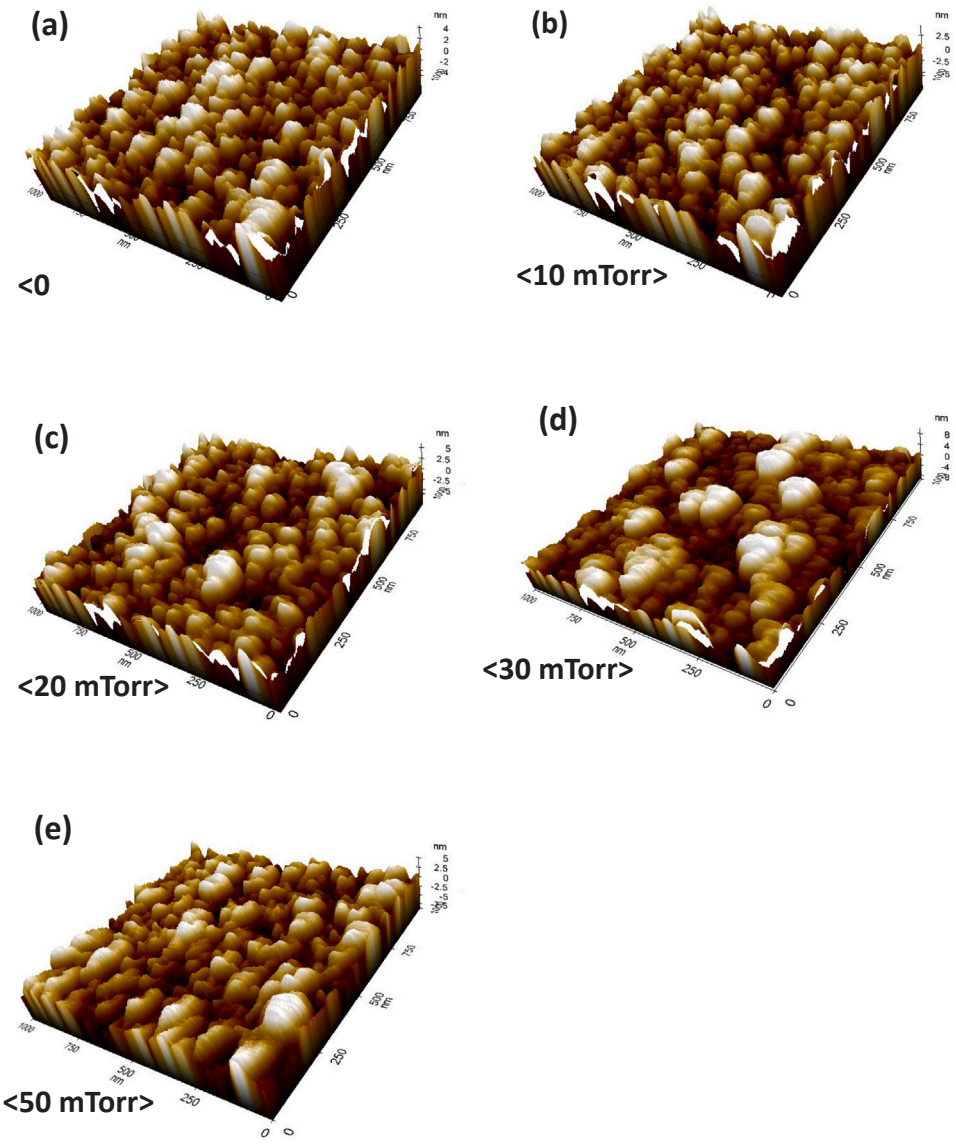

Fig. 3. Atomic Force Microscopy images of ZnO films grown on p-GaAs substrates under oxygen pressure of (a) 0, (b) 10, (c) 20, (d) 30, and (e) 50 mTorr.

can be seen in Fig. 4(a), with increasing deposition pressure from 0 to 50 mTorr, the intensity of E_1(LO) modes declines significantly and almost disappears under the oxygen pressure of 50 mTorr. One of the possible reasons is at lower oxygen pressure zinc excess caused resonance effects for LO modes in visible range due to the presence of impurity state Zinc interstitial (Zn_i) and oxygen vacancy (V_O). It is well-known that even un-doped ZnO films still can have point defects, referred to as native defects, such as oxygen vacancy V_O and interstitial zinc Zn_i, zinc vacancy V_{Zn}, interstitial oxygen O_i, and antisite oxygen O_{Zn}. Among them, V_O and Zn_i can vary ZnO from an intrinsic to n-type doping-like material [21,22]. Fig. 4(b) presents the Raman spectra in the range shift from 400 to 800 cm^{-1}. It is shown that as oxygen pressure reduces from 50 to 0 mTorr, the Raman of E_1(LO) modes red-shift from 583 to 575 cm^{-1}, respectively. Previous reports point out that great intensity of E_1(LO) modes and redshift result in serious oxygen deficiency in activated ZnO [20,23]. Moreover, in Raman spectra, the shifting of peaks is related to the chemical bond length of molecules. A shorter bond length will cause to shift to a higher wavenumber, vice versa. Therefore as increase oxygen pressure from 0 to 30 mTorr, crystallite size is larger leading to shortening the bond length and blue-shift in Raman peaks. The Raman spectra are well consistent with XRD and AFM results. Therefore, the optical properties and defect states of ZnO films grown on the p-GaAs substrate are strongly affected by the oxygen working pressure. This influence directly impacts the performance of ZnO/p-GaAs heterojunction solar cells which will be further discussed in the next part.

The schematic diagram of ZnO/p-GaAs heterojunction solar cells is shown in Fig. 5(a). Au film was grown on the back side of the GaAs wafer and Ti/Au bi-layer was evaporated on the ZnO layer by using the shadow mask to form the Ohmic contacts. Fig. 5(b) illustrates the current–voltage (I – V) curves of the photovoltaic solar cells under 1

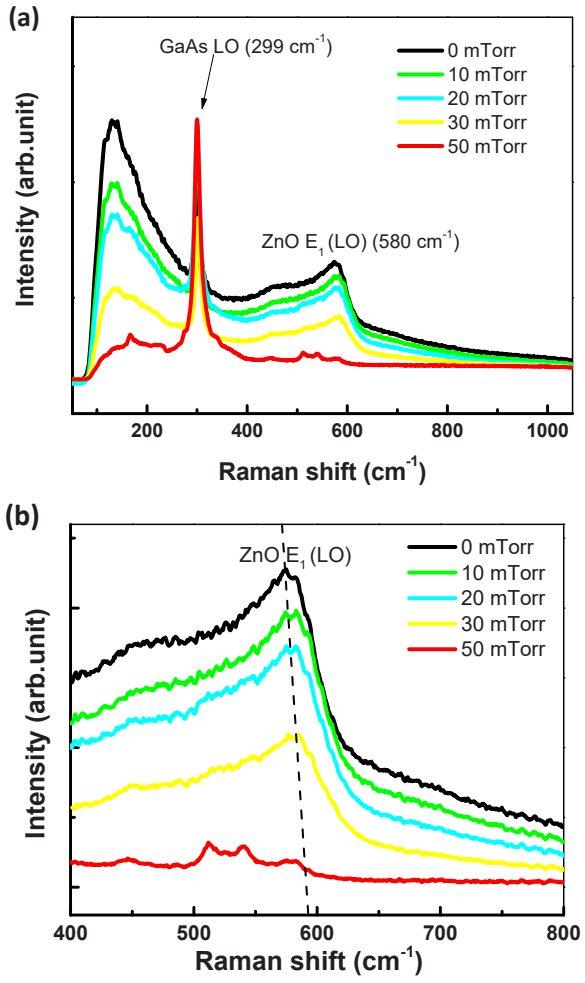

Fig. 4. (a) and (b) Raman scattering spectra of ZnO films grown on p-GaAs substrates under the various oxygen pressures.

sun illumination. J_{SC} shows an impressive enhancement from 20.6 to 25.4 mA/cm^2 as increasing oxygen flux from 0 to 20 mTorr and slightly reduces down 24.3 mA/cm^2 at 30 mTorr. Meanwhile, the value of open-circuit voltage improves from 0.490 to 0.504 with the increase of oxygen pressure from 0 to 50 mTorr. Without considering the series and shunt resistance, the fill factor (FF_0) is dependent on the open-circuit voltage as follows:

$$FF_0 = \frac{\upsilon_{OC} - \ln(\upsilon_{OC} + 0.72)}{\upsilon_{OC} + 1} \quad (1)$$

where $\upsilon_{OC} = qV_{OC}/nKT$ with V_{OC} is open-circuit voltage, n is an ideal factor, K is Boltzmann's constant, and T is measurement temperature. The solar energy conversion efficiency η is a decisive parameter for the costs and sustainability of photovoltaic production. The η of a solar cell is defined as the ratio between the power extracted at the maximum power point of the solar cell and the power of the incident sunlight illumination as follows:

$$\eta = FF_0 \frac{I_{SC}.\ V_{OC}}{P_{sun}} \quad (2)$$

Fig. 5(c) displays the value of FF_0 and η as the function of the oxygen working pressure. Here it clearly shows that the value of FF_0 slightly increases from 68.29 % to 68.84 % as oxygen from 0 to 50 mTorr, respectively. Out of five samples that have been investigated, the highest efficiency of about 8.746 % is obtained for a sample at 30 mTorr due to their high I_{SC} and V_{OC}. The efficiency of the ZnO/p-GaAs heterojunction solar cells obtained in this report is higher than that of the previous pieces of literatures [24,25]. However, this obtained efficiency is still much smaller than theoretically predicted data of 12.8 % [26] that are ascribed to the presence of some defects in the devices during the fabrication process. The enhancement of this efficiency with oxygen pressure (from 0 to 30 mTorr) may be attributed to the suppression of defects state and the improvement of the crystallinity in ZnO thin films. When we increase the oxygen pressure, the concentration of oxygen vacancy and zinc interstitial can be suppressed, and it leads to the reduction of recombination of electron-hole pairs in the defects centers. Another possible reason is as increasing the oxygen pressure from 0 to 30 mTorr, the thickness of ZnO films decreases (Fig. 2) resulting in the enhancement of the number of available photons in the space charge region and the augmentation of I_{SC} [24]. The values of I_{SC}, V_{OC}, FF_0, η under the various oxygen pressures are summarized in Table 1. Another key parameter used to judge the performance of a solar cell is external quantum efficiency (EQE). Fig. 5(d) presents the EQE spectra of ZnO/p-GaAs solar cells which were carried out in the wavelength range from 250 to 920 nm. The highest EQE is about 65 % observed in the visible range for sample grown at 20 and 30 mTorr. The changing trend of the maximum EQE is similar to the change of I_{SC} with the oxygen pressure. It is clearly shown in Fig. 5(d) that in the UV range ($\lambda < 350$ nm) the EQE is much lower than that in the visible range. This indicates the blocking action of the ZnO layer. However, a sample with the ZnO layer deposited at low oxygen pressure (0 and 10 mTorr) displays a higher EQE in the UV range. It is assumed that at low oxygen pressure, the thickness of ZnO films is higher leading to higher UV light absorption, and EQE increases. The high UV light absorption of ZnO films was reported in the previous reputed literatures [11,27]. By using UV–vis measurement, the optical bandgap of ZnO was calculated at about 3.3 eV which could contribute to the absorption in the range of light of $\lambda < 350$ nm. Therefore, considering all the key parameters and EQE spectrum, about 613 nm can be considered the optimum thickness of ZnO layer which was obtained at 30 mTorr. Moreover, EQE drops significantly within the IR wavelength of more than 900 nm. These behaviors of EQE with wavelength are further explained by carrier transport which is shown in Fig. 6.

Fig. 6(a) and (b) show the diagram structure, carrier transport, and operation mechanism of ZnO/p-GaAs solar cells at the bias voltage of 0 and 0.5, respectively. In the energy band diagram, the electron affinity and the band gap are 4.35 and 3.27 eV for ZnO and 4.07 and 1.42 eV for GaAs, respectively [28]. When operating at proper small reverse bias or 0 V (Fig. 6(a)), the 1 sun illumination on ZnO/p-GaAs heterojunction, ZnO films acts as anti-reflectance layer and transmittance in the visible range, so almost light is absorbed by p-GaAs layer generating electron-hole pairs. For photons with energy higher than the ZnO bandgap, the electron-hole pairs are generated close to the surface and recombined in the ZnO layer [29]. Therefore, illumination of high energy photons does not dominate mainly to the EQE of solar cells, and as red-shift of wavelength, EQE values increase significantly. When the light that it's

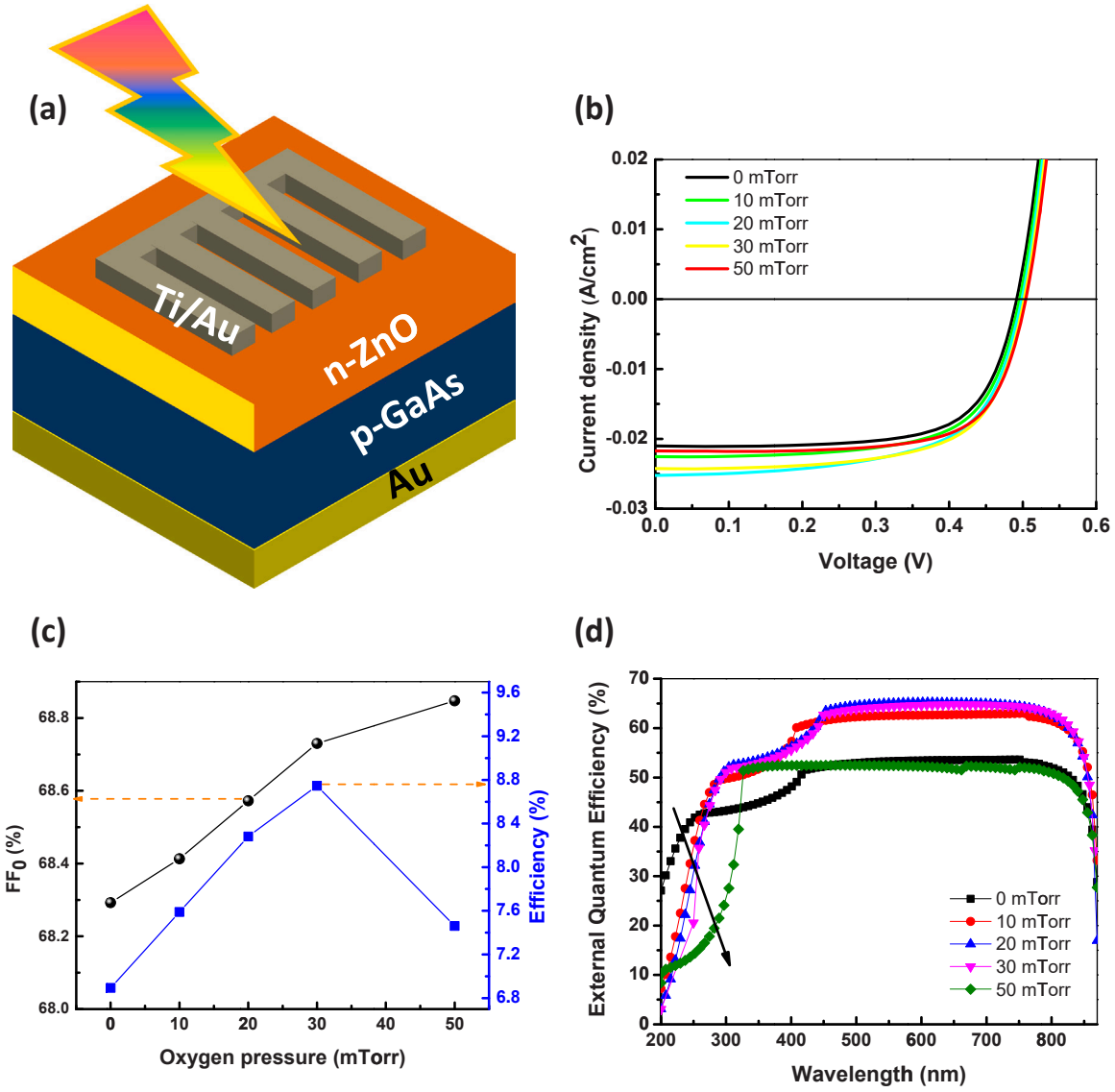

Fig. 5. (a) Schematic of fabricated metal/ZnO/p-GaAs/metal heterojunction structured solar cell, (b) current density versus voltage curves of ZnO/p-GaAs solar cell, (c) FF_0 and efficiency of ZnO/p-GaAs as a function of oxygen pressure.

Table 1
The photovoltaic parameters of the ZnO/p-GaAs heterojunction solar cells.

Sample	J_{SC} (mA/cm^2)	V_{OC} (V)	FF_0 (%)	η (%)
0 mTorr	20.6	0.49	68.29	6.89
10 mTorr	22.5	0.493	68.41	7.59
20 mTorr	25.4	0.497	68.57	8.28
30 mTorr	24.3	0.501	68.73	8.75
50 mTorr	21.5	0.504	68.85	7.46

photon energy is lower than ZnO band energy and higher than that of GaAs illuminating to solar cells, the electrons in the GaAs valance band excite to the GaAs conduction band generating electron-hole pairs. Under the electrical field, electrons in the conduction band sweep from GaAs to ZnO and holes transit reverse. This process forms the photocurrents in solar cells. Under forward bias (Fig. 6(b)), considering the valance band minima and conduction band maxima, a previous report demonstrated that the barrier for holes is about 8-fold higher than for electrons [30]. This suggested that electron injection from ZnO into p-GaAs is higher than the reverse hole injection. According to Raman, V_O and Zn_i reduced when the oxygen pressure increased; therefore, generated electrons easily captured by the trap states resulted in a reduction of the I_{SC}. The presence of higher defect density at lower oxygen pressure can suppress the free carrier, which may cause the lower performance of solar cells.

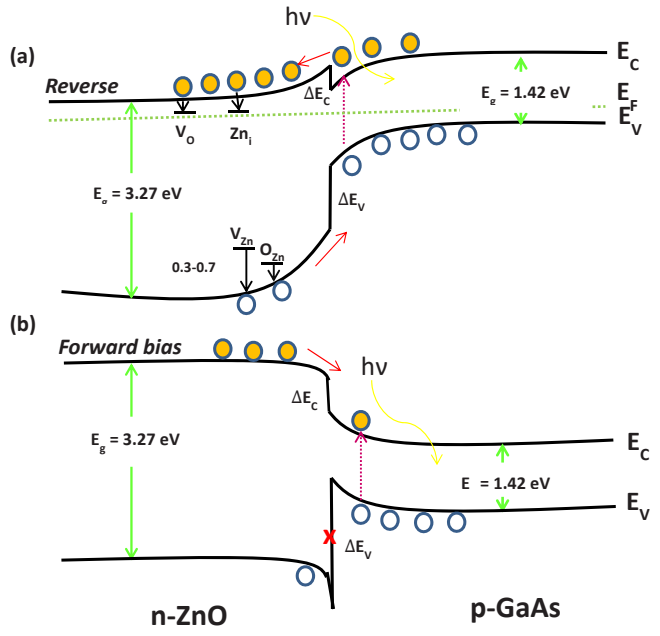

Fig. 6. Schematic diagram illustrating energy band and carrier transport mechanism in ZnO/p-GaAs solar cell under (a) reverse bias and (b) forward bias.

4. Conclusions

In conclusion, solar cells based on ZnO/p-GaAs heterojunction were fabricated by using the pulsed laser deposition method under the various oxygen pressures from 0 to 50 mTorr. We characterized the structure, morphology, and optical properties of ZnO on GaAs by XRD, AFM, and Raman, respectively. It was found that the crystallinity of ZnO films enhanced as increasing oxygen pressure from 0 to 30 mTorr and re-declined when oxygen was up to 50 mTorr. The morphology conducted by AFM confirmed this XRD data. The trap concentration was demonstrated to reduce with the increase of oxygen flux. The photovoltaic parameters are investigated for five samples, and we found that the best solar cell performance is conducted in sample fabricated under 30 mTorr. The impact of oxygen flux on the performance of ZnO/p-GaAs heterojunction was observed. This study provides a design rule for the economical product solution for high-performance solar cells.

CRediT authorship contribution statement

Thi Kim Oanh Vu: Conceptualization, Methodology, Formal analysis, Writing – original draft. **Minh Tien Tran:** Software, Project administration. **Eun Kyu Kim:** Validation, Supervision.

Data Availability

The data that has been used is confidential.

Declaration of Competing Interest

The authors declare that they have no known competing financial interests or personal relationships that could have appeared to influence the work reported in this paper.

Acknowledgements

This research was supported by the excellent research team development program grant funded by Vietnam Academy of Science and Technology (VAST) (NCXS 02.05/22-23), Vietnam, and in part supported by National Research Foundation of Korea (NRF) grant funded by the Korean government (MSIT) (NRF-2020R1A4A4078674 and 2022M3I8A2085434), the Republic of Korea.

References

[1] S. Vallisree, R. Thangavel, T.R. Lenka, Modelling, simulation, optimization of Si/ZnO and Si/ZnMgO heterojunction solar cells, Mater. Res. Express 6 (2019) 025910, https://doi.org/10.1088/2053-1591/aaf023
[2] A. Richter, M. Hermle, S.W. Glunz, Reassessment of the limiting efficiency for crystalline silicon solar cells, IEEE J. Photovolt. 3 (2013) 1184–1191, https://doi.org/10.1109/JPHOTOV.2013.2270351
[3] J. Zhu, S. Park, O.Y. Gong, C. Sohn, Z. Li, Z. Zhang, B. Jo, W. Kim, G.S. Han, D.H. Kim, T.K. Ahn, J. Lee, H.S. Jung, Formamidine disulfide oxidant as a localized electron scavenger for > 20 % perovskite solar cell modules, Energy Environ. Sci. 14 (2021) 4903–4914, https://doi.org/10.1039/D1EE01440D
[4] B.-W. Park, D.U. Lee, D. Jung, W.S. Yang, T.K.O. Vu, T.J. Shin, J. Baik, C.-C. Hwang, E.K. Kim, S.I. Seok, Long-term chemical aging of hybrid halide perovskites, Nano Lett. 19 (8) (2019) 5604–5611, https://doi.org/10.1021/acs.nanolett.9b02142
[5] J.Y. Kim, J.-W. Lee, H.S. Jung, H. Shin, N.-G. Park, High-efficiency perovskite solar cells, Chem. Rev. 120 (15) (2020) 7867–7918, https://doi.org/10.1021/acs.chemrev.0c00107
[6] C. Lin, Stabilizing organic-inorganic lead halide perovskite solar cells with efficiency beyond 20 %, Front. Chem. 3389 (2020) 00592, https://doi.org/10.3389/fchem.2020.00592
[7] O.D. Miller, E. Yablonovitch, S.R. Kurtz, Strong internal and external luminescence as solar cells approach the shockley-Queisser limit, IEEE J. Photovolt. 2 (2012) 303–311, https://doi.org/10.1109/JPHOTOV.2012.2198434
[8] M.S. Norseng, GaSelf-diffusion in isotonically enriched GaAs heterostructures doped with Si and Zn, M.S.Thesis, 1999. ⟨https://www.osti.gov/scitech/servlets/purl/760338-3NGNWz/webviewable⟩.
[9] R. Pietruszka, B.S. Witkowski, E. Zielony, K. Gwozdz, E. Placzek-Popko, M. Godlewski, ZnO/Si heterojunction solar cell fabricated by atomic layer deposition and hydrothermal methods, Sol. Energy 155 (2017) 1282–1288, https://doi.org/10.1016/j.solener.2017.07.071
[10] H.Y. Chen, H.L. Lu, L. Sun, Q.H. Ren, H. Zhang, X.-M. Ji, W.-J. Liu, S.-J. Ding, X.-F. Yang, S.W. Zhang, Realizing a facile and environmental-friendly fabrication of high-performance multicrystalline silicon solar cells by employing ZnO nanostructures and an Al_2O_3 passivation layer, Sci. Rep. 6 (2016) 38486, https://doi.org/10.1038/srep38486
[11] M. Rouchdi, E. Salmani, B. Fares, N. Hassanain, A. Mzerd, Synthesis and characteristics of Mg doped ZnO thin films: experimental and ab-initio study, Results Phys. 7 (2017) 620–627, https://doi.org/10.1016/j.rinp.2017.01.023
[12] B. Hussain, B. Kucukgok, M.Y.A. Raja, B. Klein, N. Lu, I.T. Ferguson, Is ZnO as a universal semiconductor material an oxymoron? Proc. SPIE 8987 (2014) 898718, https://doi.org/10.1117/12.2042926
[13] T.K.O. Vu, D.U. Lee, E.K. Kim, The enhancement mechanism of photo-response depending on oxygen pressure for Ga_2O_3 photodetectors, Nanotechnology 31 (2020) 245201, https://doi.org/10.1088/1361-6528/ab76f5
[14] T.K.O. Vu, D.U. Lee, E.K. Kim, Influence of titanium adhesion layer on performance of β-Ga_2O_3 solar-blind photodetector, Mater. Chem. Phys. 252 (2020) 123248, https://doi.org/10.1016/j.matchemphys.2020.123248
[15] S. Hussain, Y. Khan, V. Khranovskyy, R. Muhammad, R. Yakimova, Effect of oxygen content on the structural and optical properties of ZnO films grown by atmospheric pressure MOCVD, Prog. Nat. Sci.: Mater. Int. 23 (2013) 44–50, https://doi.org/10.1016/j.pnsc.2013.01.006
[16] C. Periasamy, R. Prakash, P. Chakrabarti, Effect of post annealing on structural and optical properties of ZnO thin films deposited by vacuum coating technique, J. Mater. Sci.: Mater. Electron. 21 (2009) 309–315, https://doi.org/10.1007/s10854-009-9912-5
[17] H.S. Kang, B.D. Ahn, J.H. Kim, G.H. Kim, S.H. Lim, H.W. Chang, S.Y. Lee, Structural, electrical, and optical properties of *p*-type ZnO thin films with Ag dopant, Appl. Phys. Lett. 88 (2006) 202108, https://doi.org/10.1063/1.2203952
[18] S.S. Kim, B.T. Lee, Effects of oxygen pressure on the growth of pulsed laser deposited ZnO films on Si (001), Thin Solid Films 446 (2004) 307, https://doi.org/10.1016/j.tsf.2003.09.057
[19] T.K.O. Vu, D.U. Lee, E.K. Kim, The effect of oxygen partial pressure on band gap modulation of Ga_2O_3 grown by pulsed laser deposition, J. Alloy. Compd. 806 (2019) 874–880, https://doi.org/10.1016/j.jallcom.2019.07.326
[20] M. Šćepanović, M. Grujić-Brojčin, K. Vojisavljević, S. Bernik, T. Srećković, Raman study of structural disorder in ZnO nanopowders, J. Raman Spectrosc. 41 (2010) 914–921 https://doi.org/10.1002/jrs.2546.
[21] S.K. Pandey, S.K. Pandey, U.P. Deshpande, V. Awasthi, A. Kumar, M. Gupta, S. Mukherjee, Effect of oxygen partial pressure on the behavior of dual ion beam sputtered ZnO thin films, Semicond. Sci. Technol. 28 (2013) 085014, https://doi.org/10.1088/0268-1242/28/8/085014
[22] L. Liu, Z. Mei, A. Tang, A. Azarov, A. Kuznetsov, Q.-K. Xue, X. Du, Oxygen vacancies: the origin of n-type conductivity in ZnO, Phys. Rev. B 93 (2016) 235305, https://doi.org/10.1103/PhysRevB.93.235305
[23] X.L. Xu, S.P. Lau, J.S. Chen, G.Y. Chen, B.K. Tay, Polycrystalline ZnO thin films on Si (100) deposited by filtered cathodic vacuum arc, J. Cryst. Growth 223 (2001) 201, https://doi.org/10.1016/j.ceramint.2003.12.156

[24] P. Caban, R. Pietruszka, K. Kopalko, B.S. Witkowski, K. Gwozdz, E. Placzek-Popko, M. Godlewski, ZnO/GaAs heterojunction solar cells fabricated by the ALD method, Optik 157 (2018) 743–749, https://doi.org/10.1016/j.ijleo.2017.11.063
[25] K.S. Lee, G. Oh, E.K. Kim, Optimization of the p^+-ZnTe layer for back contacts of ZnTe thin-film solar cells, J. Korean Phys. Soc. 69 (2016) 416–420, https://doi.org/10.3938/jkps.69.416
[26] X. Jin, N. Tang, ZnO as an anti-reflective layer for GaAs based heterojunction solar cell, Mater. Res. Express 8 (2021) 016412.
[27] L. Fang, H. Li, X. Ma, Q. Song, R. Chen, Optical properties of ultrathin ZnO films fabricated by atomic layer deposition, Appl. Surf. Sci. 15 (2020) 527, https://doi.org/10.1016/j.apsusc.2020.146818
[28] B. Hussain, A. Aslam, T.M. Khan, M. Creighton, B. Zohuri, Electron affinity and bandgap optimization of zinc oxide for improved performance of ZnO/Si heterojunction solar cell using PC1D simulations, Electronics 8 (2019) 238, https://doi.org/10.3390/electronics8020238
[29] R. Pietruszka, B.S. Witkowski, E. Zielony, K. Gwozdz, E. Placzek-Popko, M. Godlewski, ZnO/Si heterojunction solar cell fabricated by atomic layer deposition and hydrothermal method, Sol. Energy 155 (2017) 1282–1288, https://doi.org/10.1016/j.solener.2017.07.071
[30] P. Koc, S. Tekmen, A. Baltakesmez, S. Tuzemen, K. Meral, Y. Ongane, Stimulated electroluminescence emission from n-ZnO/p-GaAs:Zn heterojunctions fabricated by electro-deposition, AIP Adv. 3 (2013) 122107, https://doi.org/10.1063/1.4842635